Velocity and attenuation of wavefields generated by point sources in anisotropic viscoelastic media: asymptotic approach

Václav Vavryčuk

Geophysical Institute, Academy of Sciences of the Czech Republic, Boční II/1401, Praha 4, Czech Republic, E-mail: vv@ig.cas.cz

ABSTRACT

Asymptotic wave quantities in anisotropic viscoelastic media such as ray velocity and ray attenuation are calculated using a stationary slowness vector defined as the slowness vector that predicts the complex energy velocity parallel to a ray. The stationary slowness vector is, in general, complex-valued and inhomogeneous. Its computation involves finding two independent unit vectors, which specify the directions of its real and imaginary parts. The wave inhomogeneity affects the asymptotic quantities and complicates their computation. The critical quantities are attenuation and the Q-factor, which can significantly vary with the slowness vector inhomogeneity. If the inhomogeneity is neglected, the directional variation of attenuation and the Q-factor can distinctly be distorted. The errors can attain values commensurate to strength of velocity anisotropy, so up to tens of percent for sedimentary rocks. This applies to strongly as well as weakly attenuative media. On the contrary, the ray velocity, which defines the wavefronts and physically corresponds to the energy velocity of a high-frequency signal propagating along a ray, is almost insensitive to the slowness vector inhomogeneity and thus can be calculated in a simplified way except for media with extremely strong anisotropy and attenuation.

1. INTRODUCTION

Majority of rocks are to some extent anisotropic and attenuative. While anisotropy mainly affects directionally dependent propagation velocity of waves, attenuation controls the directionally dependent dissipation of energy and consequently the decay of wave amplitudes along the ray path. A simplest model reflecting both wave phenomena is a model of linearized viscoelastic anisotropic medium described by complex-valued frequency-dependent viscoelastic parameters (Auld 1973; Carcione 2001). This model has been so far mainly applied to propagation of plane waves (Carcione & Cavallini 1993; Shuvalov & Scott 1999; Deschamps et al. 1997; Deschamps & Assouline 2000, Červený & Pšenčík 2005, 2006; Zhu & Tsvankin 2006, 2007). In contrast to the plane-wave propagation, modelling of wavefields generated by point sources is less developed (Carcione 1994; Audoin & Gilbaud 1998; Carcione et al. 1996). The complete wavefields are usually computed using numerical methods which directly solve the wave equation (Carcione et al. 1988; Carcione 1990; Saenger & Bohlen 2004; Moczo et al. 2007), and the asymptotic wavefields using simplistic methods valid under rather strong limitations.

In this paper, I study theoretically high-frequency properties of the wavefields propagating in anisotropic viscoelastic media. Applying the steepest-descent method to the exact point source solution, I derive asymptotic wave quantities such as the ray velocity, ray attenuation, and ray quality factor. I discuss their physical meaning and show how to calculate them. On numerical examples, I demonstrate how their values can be distorted when applying a simplified approach commonly used at present (Carcione 1994; Carcione et al. 2003, Zhu & Tsvankin 2006, 2007).

In the next, real and imaginary parts of complex-valued quantities are denoted by superscripts *R* and *I*, respectively. A complex-conjugate quantity is denoted by an asterisk. The direction of a complex-valued vector $\mathbf{v}$ is calculated as $\mathbf{v}/\sqrt{\mathbf{v}\cdot\mathbf{v}}$ (the normalization condition $\mathbf{v}/\sqrt{\mathbf{v}\cdot\mathbf{v}^*}$ is not used, because it complicates generalizing some of real-valued equations to complex-valued ones). The magnitude of the complex-valued vector $\mathbf{v}$ is $\sqrt{\mathbf{v}\cdot\mathbf{v}}$. If any complex-valued vector is defined by a real-valued direction, it is called homogeneous, and if defined by a complex-valued direction, it is called inhomogeneous. In formulas, the Einstein summation convention is used for repeated subscripts.

2. PLANE WAVES IN A VISCOELASTIC ANISOTROPIC MEDIUM

Let us assume a time-harmonic plane wave described by the displacement vector

$$u_i(\mathrm{x},t)=U(\mathrm{x})g_i \exp[-i\omega(t-\mathrm{p}\cdot\mathrm{x})]\ , \tag{1}$$

where x is the position vector, U is the amplitude, g is the unit polarization vector, ω is the circular frequency, t is time. Vector p is the slowness vector defined as $\mathrm{p}=\mathrm{n}/c$, n is the slowness direction, and c is the phase velocity. Except for the position vector x, circular frequency ω and time t, all quantities are, in general, complex-valued.

2.1. Velocity, attenuation and inhomogeneity of plane waves

Since slowness vector p in equation (1) is complex-valued, it describes not only propagation velocity of plane waves, but also their attenuation and inhomogeneity. Decomposing of p, we obtain,

$$\mathrm{p}=\left[\left(V^{phase}\right)^{-1}+iA^{phase}\right]\mathrm{s}+iD^{phase}\,\mathrm{t}\ , \tag{2}$$

where V^{phase}, A^{phase} and D^{phase} are real-valued scalars called the phase velocity, phase attenuation and phase inhomogeneity. Vectors s and t are real-valued, mutually perpendicular unit vectors, s is normal to the wavefront, and t lies in the wavefront. Furthermore, we define real-valued vectors

$$\mathrm{V}^{phase}=V^{phase}\mathrm{s},\ \mathrm{A}^{phase}=A^{phase}\mathrm{s},\ \mathrm{D}^{phase}=D^{phase}\mathrm{t}\ , \tag{3}$$

called the phase velocity, phase attenuation and phase inhomogeneity vectors. These quantities are observed and measured in experiments with plane waves, and describe the propagation velocity of the wavefront, the exponential decrease of the amplitude along the normal to the wavefront, and the exponential decrease of the amplitude along the wavefront.

Emphasize that the decomposition (2) differs from those commonly used. Usually, the slowness vector is decomposed just into its real and imaginary parts called propagation and attenuation vectors (see Aki & Richards, 2002, equation 5.96; Červený & Pšenčík 2005,

equation 6). The decomposition 2 further distinguishes between the medium attenuation and wave inhomogeneity.

2.2. Viscoelastic parameters and the Christoffel tensor

The propagation of plane waves is controlled by tensor of complex-valued density-normalized viscoelastic parameters $a_{ijkl} = c_{ijkl} / \rho$. The real and imaginary parts of a_{ijkl} describe elastic and viscous properties of the medium, and their ratio, called the matrix of quality factors,

$$q_{ijkl} = -\frac{a^R_{ijkl}}{a^I_{ijkl}} \text{ (no summation over repeated indeces)}, \tag{4}$$

quantifies how attenuative the medium is. Attenuation can also be described by a scalar quantity Q called the quality factor or the Q-factor (Carcione 2000, equation 14; Chichinina *et al*. 2006, equation 27)

$$Q^{phase} = -\frac{\left(c^2\right)^R}{\left(c^2\right)^I} \ . \tag{5}$$

The supercript 'phase' highlights that Q is calculated from the complex-valued phase velocity c, and thus it primarily describes attenuation of plane waves. Obviously, the quality factor is, in general, directionally dependent in anisotropic media. Note that the definitions (4) and (5) of the quality matrix and quality factor depend on the form of the time-harmonic wave specified in equation (1). For waves with exponential factor $\exp[i\omega(t - \mathrm{p}\cdot\mathrm{x})]$, the definitions differ from equations (4) and (5) by omitting the minus sign.

Parameters a_{ijkl} are used for constructing Christoffel tensor Γ_{jk}, which is defined either in terms of the slowness direction n,

$$\Gamma_{jk}(\mathrm{n}) = a_{ijkl} n_i n_l, \tag{6}$$

or in terms of the slowness vector p,

$$\Gamma_{jk}(\mathrm{p}) = a_{ijkl} p_i p_l \ . \tag{7}$$

The slowness direction n is real-valued for homogeneous waves but complex-valued for inhomogeneous waves. The Christoffel tensor Γ_{jk} has three eigenvalues and three eigenvectors, calculated using the Christoffel equation:

$$\left(\Gamma_{jk} - G\delta_{jk}\right) g_j = 0 \ . \tag{8}$$

The eigenvalues $G(\mathrm{n})$ and $G(\mathrm{p})$ read

$$G(\mathrm{n}) = a_{ijkl} n_i n_l g_j g_k = c^2 , \tag{9}$$

$$G(\mathrm{p}) = a_{ijkl} p_i p_l g_j g_k = 1 \ , \tag{10}$$

and define phase velocity c and slowness vector p as a function of slowness direction n. The eigenvectors define polarization vectors g. The polarization vectors are normalized, so that $\mathrm{g} \cdot \mathrm{g} = 1$. From the eigenvalue $G(\mathrm{p})$ we further derive the complex energy velocity vector as

$$v_i = \frac{1}{2}\frac{\partial G}{\partial p_i} = a_{ijkl} p_l g_j g_k \ , \tag{11}$$

which is called the group velocity vector in elastic media. Vectors v and p are related by the equation,

$$\mathrm{v} \cdot \mathrm{p} = 1. \tag{12}$$

3. WAVES GENERATED BY POINT SOURCES

3.1. Exact solution

The exact Green function in unbounded, homogeneous, anisotropic viscoelastic media can be expressed in the frequency domain as the sum of regular and singular terms, $G_{kl}^{R}(\mathrm{x},\omega)$ and $G_{kl}^{S}(\mathrm{x},\omega)$, as follows (see Vavryčuk 2007, equations 11-13):

$$G_{kl}(\mathrm{x},\omega)=G^{R}_{kl}(\mathrm{x},\omega)+G^{S}_{kl}(\mathrm{x}), \tag{13}$$

$$G^{R}_{kl}(\mathrm{x},\omega)=\frac{i\omega}{8\pi^{2}\rho}\sum_{M=1}^{3}\int\limits_{\substack{S(\mathrm{n})\\ \mathrm{n}\cdot\mathrm{x}>0}}\frac{g^{(M)}_{k}g^{(M)}_{l}}{\left(c^{(M)}\right)^{3}}\exp\left(i\omega\frac{\mathrm{n}\cdot\mathrm{x}}{c^{(M)}}\right)dS(\mathrm{n})\ , \tag{14}$$

$$G^{S}_{kl}(\mathrm{x},\omega)=\frac{1}{8\pi^{2}\rho}\sum_{M=1}^{3}\int\limits_{S(\mathrm{n})}\frac{g^{(M)}_{k}g^{(M)}_{l}}{\left(c^{(M)}\right)^{2}}\delta(\mathrm{n}\cdot\mathrm{x})\,dS(\mathrm{n})\ . \tag{15}$$

Superscript M = 1,2,3 denotes the type of wave (P, $S1$ and $S2$), g is the unit polarization vector, c is the phase velocity, ρ is the density of the medium, ω is the circular frequency, $\mathrm{x}=\mathrm{N}r$ is the position vector, r is the distance of the observation point from the source, N is the ray vector, n is the unit wave normal, and S(n) is the unit sphere. The regular term is integrated over a hemisphere, defined by $\mathrm{n}\cdot\mathrm{x}>0$. The singular term is integrated over a unit circle defined by $\mathrm{n}\cdot\mathrm{x}=0$. The reduction of the surface integral to a line integral in the singular term is due to the Dirac delta function $\delta(\mathrm{n}\cdot\mathrm{x})$ in the integrand. Phase velocity c, slowness vector p, energy velocity v and polarization vector g are, in general, complex-valued and frequency dependent. Wave normal n, ray vector N, position vector x and density ρ are real-valued and do not depend on real-valued frequency ω.

The integration in formulas (14) and (15) can also be performed over slowness surface S(p). Transforming the surface element dS(n) to dS(p) (see Burridge 1967), we can write for a particular wave, P, S1 or S2 (see Vavryčuk 2007, equations 16-17),

$$G^{R}_{kl}(\mathrm{x},\omega)=\frac{i\omega}{8\pi^{2}\rho}\int\limits_{\substack{S(\mathrm{p})\\ \mathrm{p}\cdot\mathrm{x}>0}}\frac{g_{k}g_{l}}{v}\exp(i\omega\mathrm{p}\cdot\mathrm{x})\,dS(\mathrm{p})\ , \tag{16}$$

$$G^{S}_{kl}(\mathrm{x},\omega)=\frac{1}{8\pi^{2}\rho}\int\limits_{S(\mathrm{p})}\frac{g_{k}g_{l}}{v}\,\delta(\mathrm{p}\cdot\mathrm{x})\,dS(\mathrm{p})\ . \tag{17}$$

The complete Green function is then a sum of contributions for all three waves.

3.2. Asymptotic solution

Assuming high frequency ω and an observation point far from the source, singular term (17) becomes negligible and regular term 16 can be evaluated asymptotically. Applying the steepest descent method (Ben-Menahem & Singh 1981, Appendix E) to integral (16), we obtain (see Vavryčuk 2007, equation 28)

$$G_{kl}^{A}(\mathrm{x},\omega)=\frac{1}{4\pi\rho}\,\frac{g_k g_l}{v\sqrt{|K|}}\,\frac{1}{r}\,\exp\left(i\sigma_0+i\omega\,\mathrm{p}_0\cdot\mathrm{x}\right), \tag{18}$$

where

$$\sigma_0=-\frac{1}{2}\left(\varphi_1+\varphi_2\right),\ -\frac{3}{2}\pi\le\varphi_1<\frac{1}{2}\pi,\ -\frac{3}{2}\pi\le\varphi_2<\frac{1}{2}\pi\ ,$$

and p_0 is the stationary slowness vector defined as the vector predicting the complex energy velocity (11) to be homogeneous and parallel to a ray.

Formula (18) generalizes the result obtained for elastic media (Burridge 1967; Yeatts 1984; Every & Kim 1994) and holds for all shapes of the slowness surface and for all ray directions except for a vicinity of singularities on a slowness surface (see Vavryčuk 1999, 2002) and cusps edges on a wavefront, where more involved approaches are required. The complications arise because of a rapid change of polarization vectors near a singularity and because of close positions of stationary points near a cusps edge.

Quantity $K=K_1K_2$ is the Gaussian curvature of the slowness surface, K_1 and K_2 are the principal curvatures, and φ_1 and φ_2 are their phase angles. All quantities dependent on p in formula (18) are taken at stationary point p_0. Position vector $\mathrm{x}=r\mathrm{N}$, distance r, ray vector N, frequency ω, phase angles φ_1 and φ_2, and density ρ are real-valued; but polarization vector g, Gaussian curvature K, principal curvatures K_1 and K_2, energy velocity v and slowness vector p_0 are complex-valued.

The Green function (18) can be used for calculating high-frequency wavefields generated by simple forces. If a source is represented by dipoles (see Aki & Richards, 2002, equation 3.23), a high-frequency approximation of the spatial derivative of the Green function is required,

$$\frac{\partial}{x_m}\left[G_{kl}^{A}(\mathrm{x},\omega)\right]=i\omega\, p_{0m}G_{kl}^{A}(\mathrm{x},\omega)=\frac{i\omega}{4\pi\rho}\,\frac{g_k g_l p_{0m}}{v\sqrt{|K|}}\,\frac{1}{r}\exp(i\sigma_0+i\omega\mathrm{p}_0\cdot\mathrm{x})\ . \tag{19}$$

3.3. Ray velocity, attenuation and quality factor

Decomposing the complex energy velocity v into real and imaginary parts, v^R and v^I, the exponential term in formula (18) reads

$$\exp(i\omega\mathrm{p}_0\cdot\mathrm{x})=\exp\left(i\omega\frac{r}{v}\right)=\exp\left(-\omega A^{ray}r\right)\exp\left(i\omega\frac{r}{V^{ray}}\right), \tag{20}$$

where

$$V^{ray}=\frac{vv^*}{v^R}=\frac{v^Rv^R+v^Iv^I}{v^R}\ , \tag{21}$$

$$A^{ray}=-\frac{v^I}{vv^*}=-\frac{v^I}{v^Rv^R+v^Iv^I}\ . \tag{22}$$

The asterisk in (21) and (22) means the complex conjugate quantity. Since V^{ray} and A^{ray} control the propagation velocity and the amplitude decay along a ray in formula (20), we shall call them the ray velocity and ray attenuation, respectively. They are real-valued and they can be observed and measured in wavefields generated by point sources.

From real-valued ray vector N and scalars V^{ray} and A^{ray} we can define real-valued vectors

$$\mathrm{V}^{ray}=V^{ray}\mathrm{N}\ ,\ \mathrm{A}^{ray}=A^{ray}\mathrm{N}\ , \tag{23}$$

called the ray velocity and ray attenuation vectors.

To complete the definitions of the ray quantities, we can introduce the ray quality factor Q^{ray} as

$$Q^{ray} = -\frac{\left(v^2\right)^R}{\left(v^2\right)^I} \ , \tag{24}$$

where v is the complex energy velocity (11) evaluated at the stationary point p_0.

The ray velocity V^{ray}, ray attenuation A^{ray} and ray quality factor Q^{ray} have a similar physical meaning as the phase velocity V^{phase}, phase attenuation A^{phase} and phase quality factor Q^{phase}. The only difference is that the ray quantities are defined along a ray while the phase quantities are defined along a wave normal.

4. CALCULATION OF STATIONARY SLOWNESS VECTOR

Determining the stationary point p_0 is the crucial and most complicated step in calculating the asymptotic quantities in anisotropic viscoelastic media. The stationary point p_0 can be determined either by iterations or by solving a system of polynomial equations.

The iterative procedure is fast and works well provided the wavefront is free of triplications. The procedure is based on seeking a complex-valued slowness direction n, for which the complex energy velocity v is homogeneous and directed along a specified ray vector N. This represents an inversion of the following forward scheme. First, we use equation (6) to calculate Christoffel tensor $\Gamma_{jk}(\mathrm{n})$ for a specified complex-valued slowness direction n. Second, we compute its eigenvalues and eigenvectors, and construct the complex-valued slowness vector p. Third, we calculate the complex energy velocity v using formula (11). Normalizing vector v, we obtain ray vector N. When inverting this scheme, we fix a real-valued ray vector N and seek for four unknown angles: two angles define the real part and two others define the imaginary part of slowness direction n_0. The misfit function can be defined as the modulus of the complex-valued deviation between the fixed and predicted ray vectors. The inversion is non-linear and can be performed using standard methods (Press et al. 2002). Finding vector n_0, the stationary slowness vector p_0 is readily obtained using equation (10).

If the wavefront is multi-folded, the determination of stationary slowness p_0 is more involved. When using iterations, we have to be careful to find all slowness vectors corresponding to a given ray that might be sometimes tricky. The other possibility is to follow Vavryčuk (2006) and solve a system of polynomial equations in unknown components of p_0.

The stationary point p_0 is calculated from the real-valued ray vector N by solving the following equations:

$$D_{kk}N_i - a_{ijkl}D_{jk}p_{0l}p_{0m}N_m = 0, \quad i = 1, 2, 3, \tag{25}$$

where D_{jk} is the matrix of cofactors of $\hat{D}_{jk} = \Gamma_{jk} - G\delta_{jk}$,

$$\begin{aligned}
D_{11} &= (\Gamma_{22} - G)(\Gamma_{33} - G) - \Gamma_{23}^2, \quad D_{12} = D_{21} = \Gamma_{13}\Gamma_{23} - \Gamma_{12}(\Gamma_{33} - G), \\
D_{22} &= (\Gamma_{11} - G)(\Gamma_{33} - G) - \Gamma_{13}^2, \quad D_{13} = D_{31} = \Gamma_{12}\Gamma_{23} - \Gamma_{13}(\Gamma_{22} - G), \\
D_{33} &= (\Gamma_{11} - G)(\Gamma_{22} - G) - \Gamma_{12}^2, \quad D_{23} = D_{32} = \Gamma_{12}\Gamma_{13} - \Gamma_{23}(\Gamma_{11} - G),
\end{aligned} \tag{26}$$

where $\Gamma_{jk} = \Gamma_{jk}(\mathrm{p}_0)$, $G = G(\mathrm{p}_0) = 1$.

Equations (25) represent a system of coupled polynomial equations of the 6th order in unknowns p_{01}, p_{02} and p_{03}. Solving the equations we obtain a complete set of slowness vectors corresponding to all wave types and to all branches of the wave surface including the case when the wave surface is multi-folded. The equations have been originally derived for elastic media, but they can equally be applied to viscoelastic media by considering parameters a_{ijkl} to be complex-valued. Consequently, the retrieved slowness vector p_0 becomes also complex-valued.

Note that equation (25) yields also some spurious solutions which must be rejected by checking, whether the complex energy velocity vector (11) is really homogeneous for a given slowness vector solution or not. For details, see Vavryčuk (2006).

5. PHYSICAL MEANING OF RAY VELOCITY

The ray velocity V^{ray} is closely related to the so-called time-averaged energy velocity $\overline{V}^{energy}$ defined by some authors when studying energy flux of time-harmonic plane waves in viscoelastic anisotropic media (Carcione & Cavallini 1993, Carcione 2001). The time-averaged energy velocity vector is a vector describing the velocity of time-averaged energy transmitted by a plane wave and is expressed as (Červený & Pšenčík 2006, equation 35)

$$\overline{V}_i^{energy} = \frac{S_i}{E} = \frac{\left(a_{ijkl} U_k U_j^* p_l\right)^R}{\left(a_{ijkl} U_k U_j^* p_l\right)^R p_j^R} \ . \tag{27}$$

Vector S is the real part of the time-averaged energy-flux vector, and E is the real-valued time-averaged total energy density of the propagating wave. Taking into account equation (11), we obtain

$$\overline{V}_i^{energy} = \frac{\overline{v}_i^R}{\overline{v}_k^R p_k^R} , \tag{28}$$

where $\overline{\mathrm{v}}$ means the time-averaged complex energy velocity vector.

For stationary p, velocity $\overline{\mathrm{V}}^{energy}$ can further be simplified. Since $\mathrm{v} = \mathrm{N}v$ is a homogeneous vector with the direction N independent of time, the time-averaged vector $\overline{\mathrm{v}}^R$ can be substituted by the instant vector $\mathrm{v}^R = \mathrm{N}v^R$,

$$\overline{V}_i^{energy} = \frac{v_i^R}{v_k^R p_k^R} = \frac{N_i}{N_k p_k^R} \ . \tag{29}$$

Taking into account that

$$v_i p_i = 1 , \tag{30}$$

which is equivalent to

$$v_i^R p_i^R - v_i^I p_i^I = 1 , \ v_i^R p_i^I + v_i^I p_i^R = 0 \ , \tag{31}$$

we can write

$$v^R = \left(v^R v^R + v^I v^I\right) N_k p_k^R \ , \tag{32}$$

and $\overline{\mathrm{V}}^{energy}$ is finally expressed as

$$\overline{V}_i^{energy} = N_i \frac{v^R v^R + v^I v^I}{v^R} \ . \tag{33}$$

Comparing equations (21) and (23) with (33) we can see that the time-averaged energy velocity vector $\overline{\mathrm{V}}^{energy}$ for p being stationary yields exactly the same value as the ray velocity vector V^{ray}. Hence, the main difference between the ray and energy velocities is that the energy velocity is defined for any complex-valued p, but the ray velocity is defined just for stationary p. For a stationary wave, both velocities have the same physical meaning.

Note that the stationary wave displays also other interesting properties. In viscoelastic anisotropic media, the instant energy flux of a harmonic plane wave has, in general, a time-dependent direction. For a stationary wave, the instant energy flux direction is constant.

6. NUMERICAL EXAMPLES

In this section, I demonstrate properties of ray velocity and ray attenuation on numerical examples performed for P waves. I show the differences produced by different definitions of propagation velocities and attenuations. I adopted four transversely isotropic viscoelastic models with a different strength of anisotropy and attenuation (see Tables 1 and 2). Their values are chosen to lie within the limits of observations for sedimentary rocks. The frequency of the signal is assumed to be 30 Hz.

The four models used (A, B, C and D) basically combine two models of velocity anisotropy and two levels of attenuation. The *P*-wave anisotropy is 23% for models A and B, and 11% for models C and D (see Table 3). The models A and B differ in the level of attenuation, which is twice larger for model A than for model B. The same applies to models C and D. The attenuation anisotropy is 68% for models A and B, and 58% for models C and D. The *Q*-factor anisotropy is 48% for all four models.

Figure 1 shows the directional variations of phase and ray velocities, attenuations and *Q*-factors for model A for angles between 0° and 90°. The velocities, attenuations and *Q*-factors are calculated using two approaches: first, a correct method described in Sections 3 and 4 and based on evaluating the velocities from the stationary slowness vector p_0; and second, a simplified method based on evaluating the velocities from a homogeneous slowness vector p.

The figure shows that the velocities calculated using the two methods coincide the differences between them being within the width of the line. The same result is obtained when attenuation is neglected at all. Hence the attenuation of the models studied is not so high to affect the velocities considerably. The errors in phase and ray velocities produced using the simplified non-stationary method are about 0.05% or less (see Table 4). However, the errors in the attenuations and Q-factors produced by the simplified method are more significant and clearly visible (see Figure 1c-f). They attain values of 17.4% and 16.6% for the phase and ray attenuations, and 28.3% and 30.9% for the phase and ray Q-factors, respectively (see Table 4). Such differences cannot be neglected and point to the necessity of considering the proper stationary solution method in attenuation studies.

Table 1. Viscoelastic parameters in the standard notation

Model	Elastic parameters				Attenuation parameters			
	A_{11}^R [km^2/s^2]	A_{13}^R [km^2/s^2]	A_{33}^R [km^2/s^2]	A_{44}^R [km^2/s^2]	Q_{11}	Q_{13}	Q_{33}	Q_{44}
A	14.4	4.50	9.00	2.25	30	15	20	15
B	14.4	4.50	9.00	2.25	60	30	40	30
C	10.8	3.53	9.00	2.25	30	15	20	15
D	10.8	3.53	9.00	2.25	60	30	40	30

The two-index Voigt notation is used for density-normalized elastic parameters a_{ijkl}^R and quality-factor matrix q_{ijkl}.

Table 2. Viscoelastic parameters in the Thomsen-style notation

Model	Elastic parameters				Attenuation parameters			
	V_{P0} [km/s]	V_{S0} [km/s]	ε	δ	A_{P0} [10^{-2}]	A_{S0} [10^{-2}]	ε_Q	δ_Q
A	3.00	1.50	0.30	0.00	2.50	3.33	-0.333	0.667
B	3.00	1.50	0.30	0.00	1.25	1.67	-0.333	0.667
C	3.00	1.50	0.10	-0.10	2.50	3.33	-0.333	0.511
D	3.00	1.50	0.10	-0.10	1.25	1.67	-0.333	0.511

For the definition of parameters in the Thomsen-style notation, see Thomsen (1986) and Zhu & Tsvankin (2006).

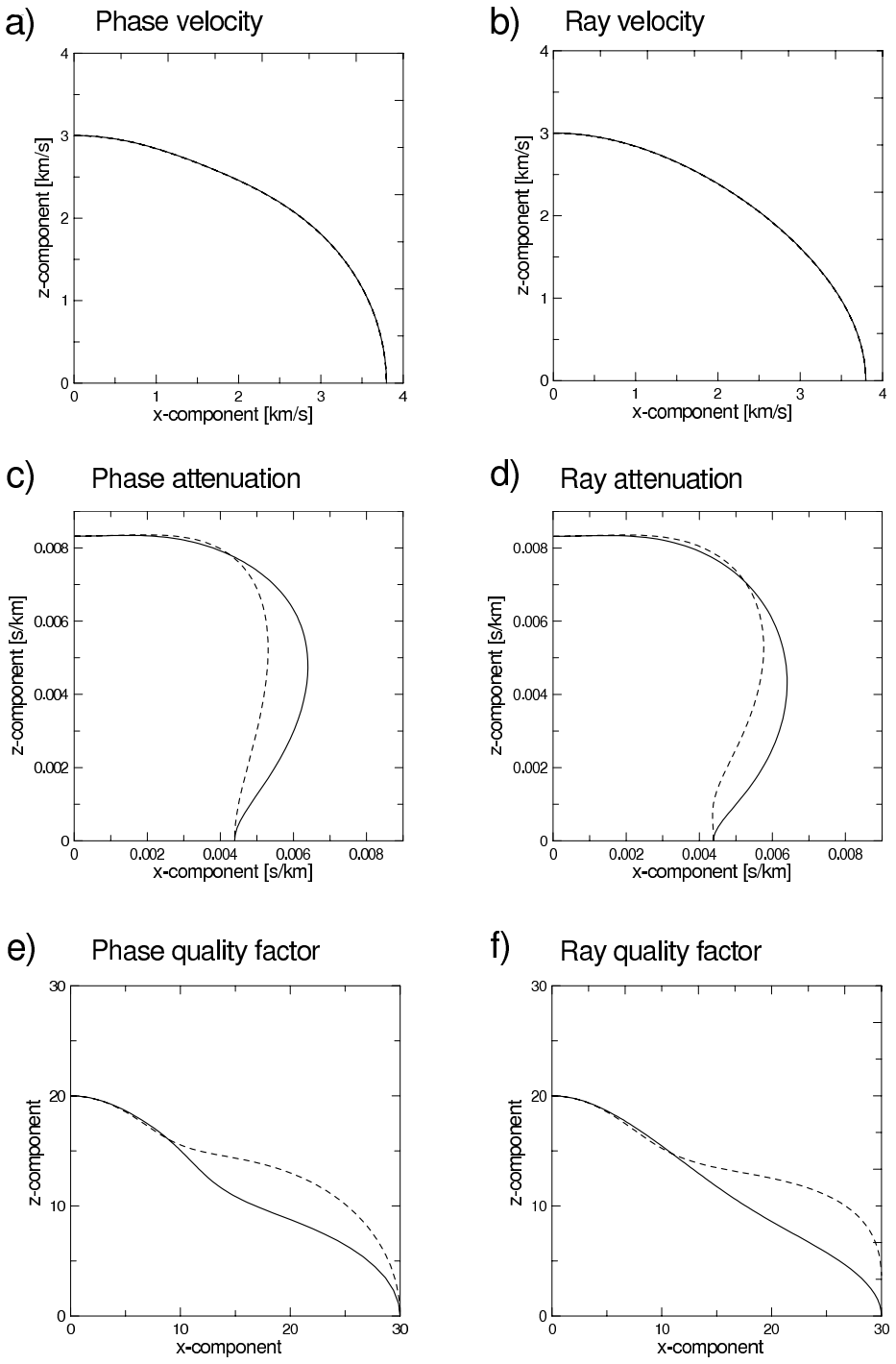

Figure 1. Polar plots of the *P*-wave velocities (a-b), attenuations (c-d) and *Q*-factors (e-f) in model A. Solid line – stationary approach (the slowness vector is inhomogeneous), dashed line – non-stationary approach (the slowness vector is homogeneous). For parameters of the model, see the text.

Figure 2 shows the velocities and attenuations for model C. Again, no visible differences are observed in velocities, when applying the stationary and non-stationary methods. However, the differences in attenuations and *Q*-factors are significant and attain values of 10.8% and 11.2% for phase and ray attenuations, and 15.4% and 16.6% for the phase and ray *Q*-factors, respectively.

Table 3. *P*-wave velocity and attenuation anisotropy

Model	$\overline{V}^{ray}$ [km/s]	a_V^{ray} [%]	$\overline{A}^{ray}$ [s/km]	a_A^{ray} [%]	$\overline{Q}^{ray}$	a_Q^{ray} [%]
A	3.28	23.3	$75.2 \cdot 10^{-4}$	67.7	21.1	48.1
B	3.27	23.4	$37.7 \cdot 10^{-4}$	67.8	42.2	48.1
C	3.06	10.5	$78.8 \cdot 10^{-4}$	58.0	21.3	48.3
D	3.06	10.5	$39.5 \cdot 10^{-4}$	58.0	42.6	48.3

$\overline{V}^{ray}$, $\overline{A}^{ray}$ and $\overline{Q}^{ray}$ are the mean *P*-wave ray velocity, attenuation and *Q*-factor; a_V^{ray}, a_A^{ray} and a_Q^{ray} are the *P*-wave ray velocity anisotropy, attenuation anisotropy and *Q*-factor anisotropy. The anisotropy is calculated as $a = 200\left(U_{MAX} - U_{MIN}\right)/\left(U_{MAX} + U_{MIN}\right)$, where U_{MAX} and U_{MIN} are the maximum and minimum values of the respective quantity.

Table 4. Maximum errors of the non-stationary approach

Model	Error V^{phase} [%]	Error V^{ray} [%]	Error A^{phase} [%]	Error A^{ray} [%]	Error Q^{phase} [%]	Error Q^{ray} [%]
A	$1.5 \cdot 10^{-2}$	$5.3 \cdot 10^{-2}$	17.4	16.6	28.3	30.9
B	$0.4 \cdot 10^{-2}$	$1.4 \cdot 10^{-2}$	17.4	16.7	28.3	31.0
C	$1.5 \cdot 10^{-2}$	$4.5 \cdot 10^{-2}$	10.8	11.2	15.4	16.6
D	$0.4 \cdot 10^{-2}$	$1.1 \cdot 10^{-2}$	10.9	11.3	15.4	16.7

The error for a particular ray is calculated as $E = 100\left|U^{exact} - U^{aprox}\right|/U^{exact}$, where U^{exact} and U^{aprox} are exact and approximate values of the respective quantity. The presented values are maxima over all rays.

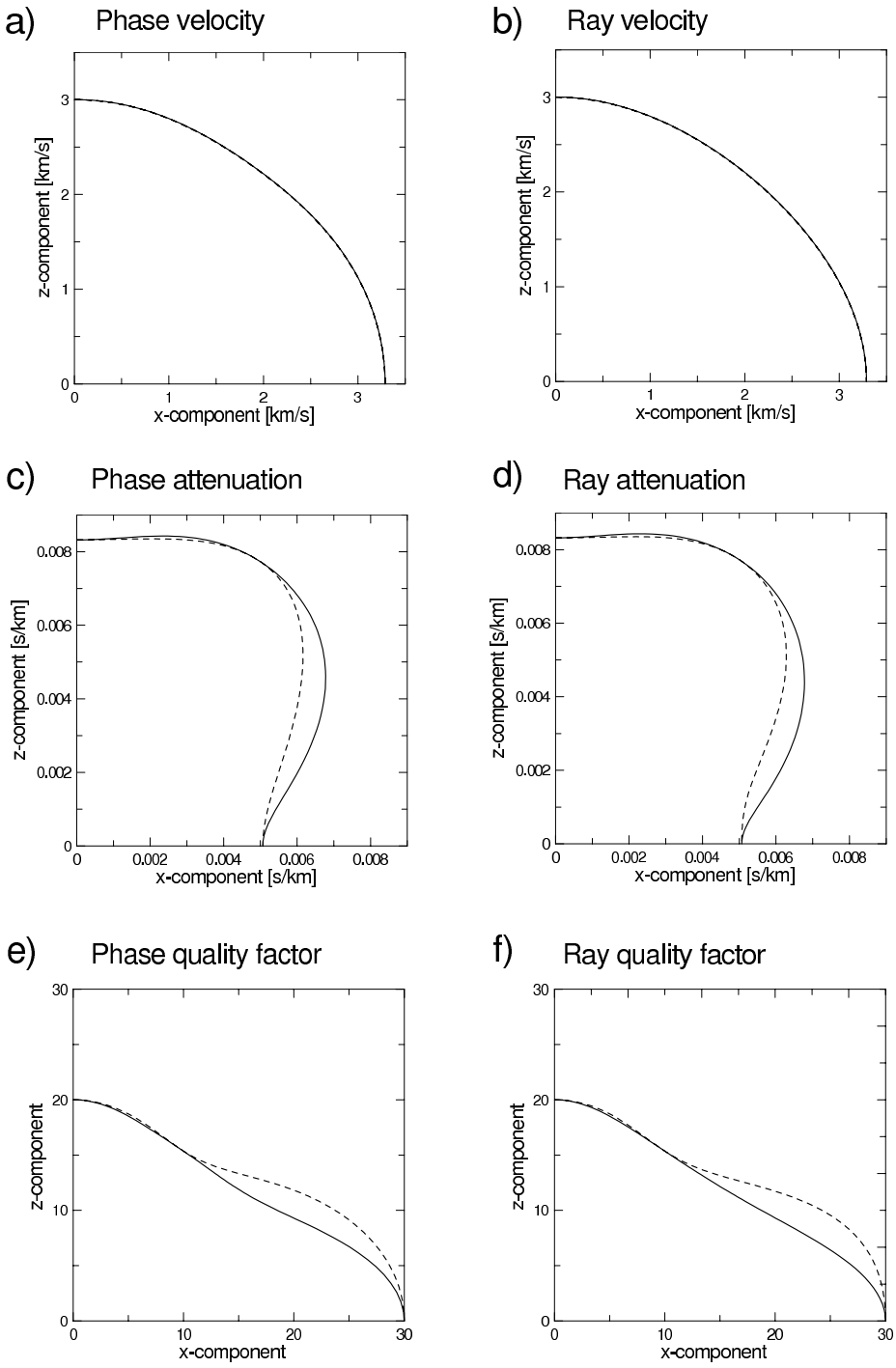

Figure 2. Polar plots of the *P*-wave velocities (a-b), attenuations (c-d) and *Q*-factors (e-f) in model C. For details, see the caption of Figure 1.

The directional variations of velocities and attenuations for models B and D are almost identical to those for models A and C, hence I do not present them. The only difference between models A and B is that the attenuation and *Q*-factor plots for model B would be of a scale twice less than for model A. The scale of velocity plots and shape of velocity, attenuation and *Q*-factor functions remains unchanged. The same applies to differences between models C and D.

Figure 3 shows the inhomogeneity of a stationary slowness vector as a function of a ray direction for models under study. The inhomogeneity is quantified by the imaginary part of the phase angle $\theta = \theta^R + i\theta^I$ which defines the complex-valued slowness direction n:

$$\mathrm{n} = \begin{bmatrix} \sin\theta\cos\varphi \\ \sin\theta\sin\varphi \\ \cos\theta \end{bmatrix}. \tag{34}$$

For a simplified non-stationary approach, angle θ is real-valued, but for a stationary approach, it is complex-valued. As seen from Figure 3, the imaginary part of θ is very small for stationary approach. Its absolute value is less than 1.2° for models A and C (more attenuative models), and even less than 0.6° for models B and D (less attenuative models). Hence, with decreasing attenuation, the imaginary part of angle θ decreases. Nevertheless, even such tiny differences between the stationary and non-stationary slowness directions are visible at phase and ray attenuation plots (see Figures 1 and 2).

The differences between the stationary and non-stationary approaches can also be exemplified on wave amplitudes. Figure 4 shows the radiation pattern for an explosion buried in models A and B plotted in the *x*-*z* plane. The explosion is characterized by the moment tensor:

$$M_{kl} = M_0 \begin{bmatrix} 1 & & \\ & 1 & \\ & & 1 \end{bmatrix}, \tag{35}$$

and the amplitude *R* of the radiated wave is calculated for observation points at a fixed distance from the explosion source using the formulas:

$$R = \sqrt{u_i u_i^*}\ ,\ u_i = M_{kl} * G_{ik,l}^A , \tag{36}$$

where M_0 is the scalar moment.

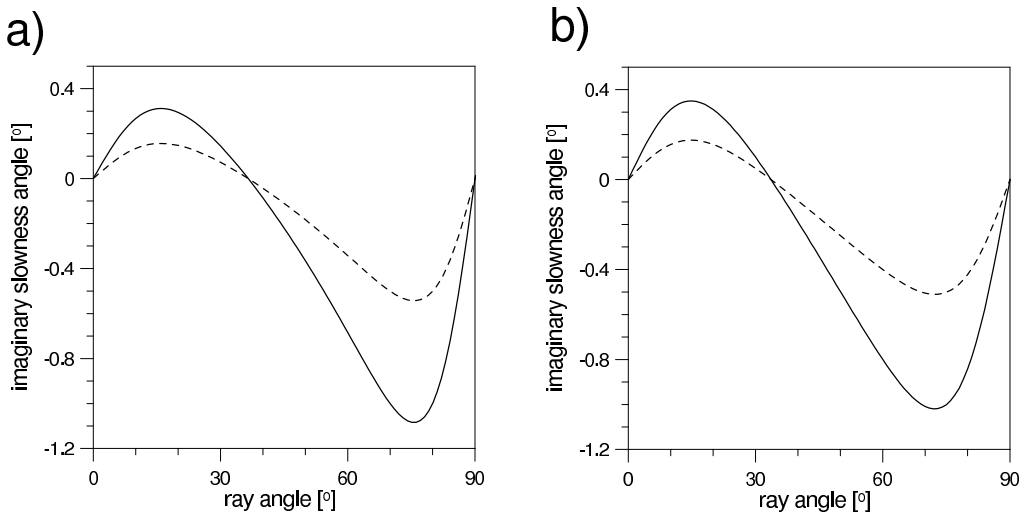

Figure 3. Imaginary part of the stationary slowness angle as a function of the ray angle. (a) Full line – model A, dashed line – model B. (b) Full line – model C, dashed line – model D. The imaginary part of the non-stationary slowness angle is identically zero for all models.

Figure 4 illustrates several interesting characteristics of the radiated waves. First, it indicates that the radiation pattern in a medium displaying velocity anisotropy can significantly deviate from the spherical pattern known for an explosion in isotropy (Figure 4, left-hand plots). Second, the departure from the spherical radiation pattern is further amplified owing to directionally dependent attenuation (Figure 4, right-hand plots). Under elastic anisotropy or anisotropy with isotropic attenuation, the radiation pattern can be non-spherical but it cannot change with increasing distance. On the contrary, we observe a strong dependence of the radiation pattern on distance from the source in Figure 4. Third, errors of wave amplitudes calculated using the non-stationary approach increase with increasing distance. Obviously, the

errors also depend on the level of attenuation, being more pronounced for more attenuative models.

Note that plots for models C and D are not presented because they are similar to those in Figure 4.

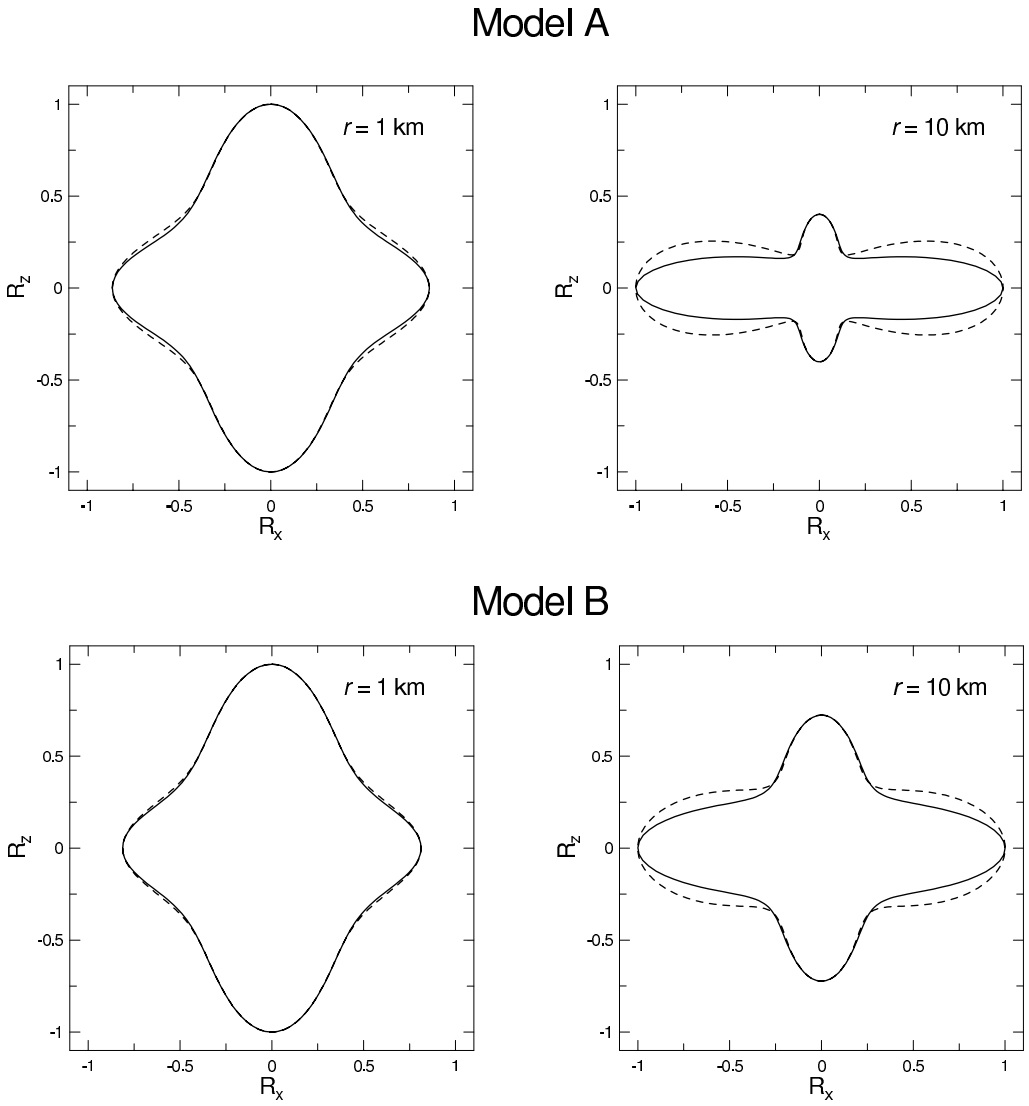

Figure 4. Radiation pattern of an explosion situated in model A (upper plots) and model B (lower plots). The wave amplitudes are calculated at distance from the source: r = 1 km and r = 10 km. Full line – stationary approach, dashed line – non-stationary approach. The radiation patterns are plotted in the x-z plane and normalized to its maximum amplitude.

7. DISCUSSION

The observation of discrepancies in attenuation calculated for homogeneous and inhomogeneous waves is rather surprising and not expected. So far, only a non-stationary approach has been applied and published in the literature (Carcione et al. 2003; Zhu & Tsvankin 2006, 2007). It was expected that the approach is satisfactory at least for low attenuation. For example, Zhu & Tsvankin (2006, 2007) argue that for low attenuation media, the inhomogeneity of the stationary slowness vector must be low. Consequently, the inhomogeneity effects must be of a second order and thus negligible. However, the above numerical examples indicate that the problem is more involved. Even though the inhomogeneity of the stationary slowness vector is low, it can produce significant effects in attenuation. The reason is that the inhomogeneity of the slowness vector is not controlled only by attenuation of the medium but also by velocity anisotropy of the medium. Hence the effects of inhomogeneous slowness vector do not necessarily decrease with decreasing attenuation.

8. CONCLUSIONS

The asymptotic evaluation of wavefields in anisotropic viscoelastic media display some substantial differences compared with that in elastic media. The correct asymptotic wave quantities must be calculated using a stationary slowness vector $\mathbf{p}_0$. This vector is defined as the slowness vector that predicts the complex energy velocity vector parallel to a ray. Since the ray direction is real, the complex energy velocity vector is homogeneous. Consequently, the stationary slowness vector $\mathbf{p}_0$ is, in general, inhomogeneous and its computation involves finding two independent unit vectors, which specify the directions of its real and imaginary parts. The stationary slowness vector can be calculated either using an iterative inversion or using a system of coupled polynomial equations of the 6^{th} order. The iterative approach is safe and advantageous when anisotropy is free of triplications. In anisotropy with triplications, the latter approach is preferable. Once we have found the stationary slowness vector, we can readily calculate the polarization vectors, phase and ray velocities, attenuations and Q-factors. Calculating the stationary slowness vectors for all ray directions, we can construct the slowness, velocity and attenuation surfaces. The most important surface is the ray velocity surface, because it defines wavefronts, and the ray attenuation surface because it can be

constructed from attenuation measurements performed on wavefields generated by point sources.

Numerical modelling indicates that asymptotic wave quantities are differently sensitive to the inhomogeneity of the stationary slowness vector $\mathbf{p}_0$. For example, the phase and ray velocities are much less sensitive than the phase and ray attenuations and Q-factors. When calculating the approximate attenuation and Q-factors using a homogeneous slowness vector $\mathbf{p}$, the errors can attain values commensurate to strength of velocity anisotropy. Hence, for anisotropy observed for sedimentary rocks they can be up to tens of percent. This applies not only to strongly attenuative media but also to weakly attenuative media.

ACKNOWLEDGEMENTS

I thank T. Chichinina and three anonymous reviewers for their helpful reviews. The work was supported by the Grant Agency of the Czech Republic, Grant No. 205/05/2182, by the Consortium Project "Seismic Waves in Complex 3-D Structures", and by the EU Consortium Project IMAGES "Induced Microseismics Applications from Global Earthquake Studies", Contract No. MTKI-CT-2004-517242. A part of the work was done while the author was a visiting researcher at the Schlumberger Cambridge Research, Cambridge, U.K.

REFERENCES

Aki, K., and P.G. Rishcards, 2002, Quantitative Seismology: University Science Books, Sausalito, California.

Audoin, B., and S. Guilbaud, 1998, Acoustic waves generated by a line source in a viscoelastic anisotropic medium: Applied Physics Letters, 72, 774-776.

Auld, B.A., 1973, Acoustic Fields and Waves in Solids: Wiley, New York.

Ben-Menahem, A., and S.J. Singh, 1981, Seismic Waves and Sources: Springer-Verlag, New York.

Burridge R., 1967, The singularity on the plane lids of the wave surface of elastic media with cubic symmetry: The Quarterly Journal of Mechanics and Applied Mathematics, 20, 41-56.

Carcione, J.M., 1990, Wave propagation in anisotropic linear viscoelastic media: theory and simulated wavefields: Geophysical Journal International, 101, 739-750. Erratum: 1992, 111, 191.

Carcione, J.M, 1994, Wavefronts in dissipative anisotropic media: Geophysics, 59, 644-657.

Carcione, J.M., 2000, A model for seismic velocity and attenuation in petroleum source rocks: Geophysics, 65, 1080-1092.

Carcione, J.M., 2001, Wave Fields in Real Media: Wave Propagation in Anisotropic, Anelastic and Porous Media: Pergamon, Amsterdam.

Carcione, J.M., and F. Cavallini, 1993, Energy balance and fundamental relations in anisotropic-viscoelastic media: Wave Motion, 18, 11-20.

Carcione, J.M., K. Helbig, and H.B. Helle, 2003, Effects of pressure and saturating fluid on wave velocity and attenuation in anisotropic rocks: International Journal of Rock Mechanics and Mining Sciences, 40, 389-403.

Carcione, J.M, D. Kosloff, and R. Kosloff, 1988, Wave propagation simulation in anisotropic (transversely isotropic) medium: The Quarterly Journal of Mechanics and Applied Mathematics., 41, 320-345.

Carcione, J.M., G. Quiroga-Goode, and F. Cavallini, 1996, Wavefronts in dissipative anisotropic media: comparison of the plane wave theory with numerical modeling: Geophysics, 61, 857-861.

Červený, V., and I. Pšenčík, 2005, Plane waves in viscoelastic anisotropic media – I. Theory: Geophysical Journal International, 161, 197-212.

Červený, V., and I. Pšenčík, 2006, Energy flux in viscoelastic anisotropic media: Geophysical Journal International, 166, 1299-1317.

Chichinina, T., V. Sabinin, and G. Ronquillo-Jarillo, 2006, QVOA analysis: *P*-wave attenuation anisotropy for fracture characterization, Geopysics, 71, No. 3, C37-C48.

Deschamps, M., and F. Assouline, 2000, Attenuation along the Poyinting vector direction of inhomogeneous plane waves in absorbing and anisotropic solids: Acustica, 86, 295-302.

Deschamps, M., B. Poirée, and O. Poncelet, 1997, Energy velocity of complex harmonic plane waves in viscous fluids: Wave Motion, 25, 51-60.

Every A.G., and K.Y. Kim, 1994, Time domain dynamic response functions of elastically anisotropic solids: Journal of Acoustical Society of America, 95, 2505-2516.

Moczo, P., J.O.A. Robertsson, and L. Eisner, 2007, The Finite-Difference Time-Domain Method for Modelling of Seismic Wave Propagation: In Advances in Wave Propagation in

Heterogeneous Earth, 421-516, Wu, R.-S., Maupin, V., eds., Advances in Geophysics 48, Dmowska, R., ed., Elsevier – Academic Press, doi: 10.1016/S0065-2687(06)48008-0.

Norris, A.N., 1994, Dynamic Green's functions in anisotropic piezoelectric, thermoelastic and poroelastic solids: Proceedings of the Royal Society of London, A. 447, 175-188.

Press, W.H., S.A. Teukolsky, W.T. Vetterling, and B.P. Flannery, 2002, Numerical Recipes: The Art of Scientific Computing: Cambridge University Press.

Saenger, E.H., and T. Bohlen, 2004, Finite-difference modeling of viscoelastic and anisotropic wave propagation using the rotated staggered grid: Geophysics, 69, 583-591.

Shuvalov, A.L., and N.H. Scott, 1999, On the properties of homogeneous viscoelastic waves: The Quarterly Journal of Mechanics and Applied Mathematics, 52, 405-417.

Thomsen, L., 1986, Weak elastic anisotropy: Geophyics, 51, 1954-1966.

Vavryčuk, V., 1999, Properties of S waves near a kiss singularity: a comparison of exact and ray solutions: Geophysical Journal International, 138, 581-589, doi:10.1046/j.1365-246X.1999.00887.x..

Vavryčuk, V., 2002, Asymptotic elastodynamic Green function in the kiss singularity in homogeneous anisotropic solids: Studia Geophysica et Geodaetica, 46, 249-266, doi: 10.1023/A:1019854020095.

Vavryčuk, V., 2006, Calculation of the slowness vector from the ray vector in anisotropic media: Proceedings of the Royal Society, A 462, 883-896.

Vavryčuk, V., 2007, Exact and asymptotic Green functions in homogeneous anisotropic viscoelastic media: this report.

Wang, C.-Y., and J.D. Achenbach, 1994, Elastodynamic fundamental solutions for anisotropic solids: Geophysical Journal International, 118, 384-392.

Willis, J.R., 1980, A polarization approach to the scattering of elastic waves. I. Scattering by a single inclusion: Journal of Mechanics and Physics of Solids, 28, 287-305.

Yeatts F.R., 1984, Elastic radiation from a point source in an anisotropic medium: Physical Review B, 29, 1674-1684.

Zhu, Y., and I. Tsvankin, 2006, Plane-wave propagation in attenuative transversely isotropic media: Geophysics, 71, T17-T30.

Zhu, Y., and I. Tsvankin, 2007, Plane-wave attenuation anisotropy in orthorhombic media: Geophysics, 72, D9-D19.